geographical analysis

Geographical Analysis (2016) **48,** 18–42

Modeling Visit Probabilities within Network-Time Prisms Using Markov Techniques

Ying Song[1], Harvey J. Miller[1], Xuesong Zhou[2], David Proffitt[3]

[1]Department of Geography, The Ohio State University, Columbus, OH, USA, [2]School of Sustainable Engineering and the Built Environment, Arizona State University, Tempe, AZ, USA, [3]Department of City and Metropolitan Planning, University of Utah, Salt Lake City, UT, USA

The space-time prism is a key concept in time geography that captures both spatial and temporal constraints on an object's potential mobility. For mobility within transportation networks, network-time prisms (NTPs) delimit accessible locations with respect to time given scheduling constraints, movement constraints, and speed limits imposed by the network. The boundary of a NTP has been used as a measure of individuals' accessibility within a network. However, the interior structure has lacked quantitative characterization, including the distribution of visit probabilities at accessible locations. This article models visit probabilities within NTPs using two types of Markov techniques: (1) Brownian motion on undirected graphs for nonvehicular mobility (e.g., walking) and (2) continuous-time semi-Markov process for vehicular mobility (e.g., biking, driving). Based on these methods, we simulate nonvehicular and vehicular visit probabilities and visualize these distributions. For vehicular mobility, we compare the simulated visit probabilities with empirical probabilities derived from trajectories collected by Global Positioning System (GPS) in New York City, USA. The visit probabilities provide a quantitative description of individuals' potential mobility within a NTP and a foundation for developing the refined accessibility benefit and cost measures that go beyond the binary nature of classical NTPs.

Introduction

The *space-time prism* (STP) is a central concept in time geography that captures both spatial and temporal constraints on an object's potential mobility. Given two known locations in geographic space, the time budget for moving, and the maximum achievable moving speeds, a STP delimits all locations that can be reached by the moving object and extra time available at each location (Hägerstrand 1970; Thrift and Pred 1981). For movements within spatial networks such as transportation infrastructure, *network-time prisms* (NTPs) account for additional constraints such as geometry, connectivity, direction restrictions, turn restrictions, and speed limits (Miller 1991; Kuijpers and Othman 2009). The prism has been widely used to model individual constraints on

Correspondence: Ying Song, Department of Geography, The Ohio State University, 1036 Derby Hall/154 N. Oval Mall, Columbus, OH 43210
e-mail: song.851@osu.edu

Submitted: July 9, 2014. Revised version accepted: December 1, 2014.

doi: 10.1111/gean.12076

activity-based travel demand (e.g., McNally 2000; Bowman and Ben-Akiva 2001; Dong et al. 2006) and create people-based measures for individuals' accessibility to the environment and the opportunities within that environment (e.g., Kwan 1998; O'Sullivan, Morrison, and Shearer 2000).

The STPs and NTPs in their classic forms are binary measures: all locations and times within the prism are considered to be equally accessible. Recent investigations into the planar STP suggest that this binary conceptualization masks intricate properties of the prism interior. In particular, it is apparent that the probabilities to visit locations within a STP are unequal: locations toward the center are more likely to be visited since there is more time available at those locations (and therefore more possible paths through those locations) relative to locations near the boundary (Winter and Yin 2010a, b; Song and Miller 2014).

This article develops methods for modeling visit probabilities within NTPs. We adapt Markov processes and develop techniques according to two basic types of movements: (1) Brownian motion on undirected graphs for nonvehicular mobility that is loosely constrained by the network (such as walking) and (2) semi-Markov processes for vehicular mobility that is tightly constrained by the network (such as bicycling and driving). To illustrate our methods, we simulate NTP visit probabilities for the New York City, USA, street network and compare the simulated vehicular visit probabilities to empirical probabilities derived from trajectory data collected by a commercial navigation vendor using Global Positioning System (GPS).

Our choice of Markov processes to model NTP visit probabilities is a direct extension of the planar STP visit probability methods pioneered by Winter and Yin (2010a, b) and refined by Song and Miller (2014). Winter and Yin (2010a, b) treat planar space and time as discrete and use random walks (RWs) to model STP visit probabilities while Song and Miller (2014) use Brownian motion as the limiting case of RWs in continuous space and time. The RW/Brownian approach is in the spirit of time geography since this is a theory of the physical limits on accessibility, not a behavioral theory, although it can be used as input to behavioral transportation models (Pred 1977; Ellegård and Svedin 2012). RWs and Brownian motion are fundamental physical models of movement that can be made consistent with STP constraints; Markov processes generalize this approach for NTPs. We focus on extending analytical time geography to the prism interior structure; therefore, our methods model NTP visit probabilities based on the intrinsic physical properties of the prism without additional behavioral assumptions or models. Extending the STP and NTP visit probability methods to incorporate spatial behavior is a research frontier beyond the scope of this current article.

In addition to continuing the development of analytical time geography, the methods in this article also have practical applications. Although our visit probability methods focus on the intrinsic properties of NTPs, they include parameters that can be calibrated to maximize the fit between the simulated visit probability distribution and empirical observations of movement behavior. Our methods can also incorporate real-time traffic conditions by adjusting the maximum achievable moving speeds (or delays due to congestions) within the networks. Modeling NTP visit probability distributions can allow the refinement of prism-based accessibility measures that are based on a binary conceptualization of the prism (e.g., Kwan 1998; Miller 1999). Furthermore, since the range of possible speeds varies by location in the prism, knowing the visit probability distribution allows calculation the *potential speed distribution* within a prism. This facilitates linking the prism to speed-related mobility properties such as fuel consumption, tailpipe emissions, and safety (Shibata and Fukuda 1994; Barth et al. 1996; Ahn et al. 2002). We discuss some of these applications in more detail in the concluding section.

The rest of the article is organized as follows. The next section provides background by discussing analytical time geography and modeling visit probabilities within STPs. The subsequent section presents the methodology: the Markovian techniques of Brownian motion and semi-Markov processes to model movement probabilities within NTPs for nonvehicular and vehicular mobility, respectively. The results section illustrates the methodology by simulating and visualizing movement probabilities for two scenarios: walking in Manhattan and driving across Manhattan. We chose the Manhattan borough of New York City due to the availability of a mobility data set from a commercial navigation service. For the vehicular mobility case, we calibrate the network mobility level using this data set, simulate movement probabilities, and compare them with empirical probabilities derived from these data. The article concludes with a discussion of future research.

Background

Analytical time geography

Time geography represents an individual's actual and potential mobility as *space-time paths* and *STPs*, respectively (Hägerstrand 1970; Lenntorp 1977). Fig. 1a shows a space-time path that traces an individual's movements through time and space. Each vertical tube represents an activity location and its availability in time (e.g., a grocery store open from 7:00 am to 11:00 pm). In order to participate in activities sparsely distributed in time and space, an individual has to trade time for movement among activity locations. The slope of the space-time path is the ratio of distance to time; this is the speed of moving individual. The steeper the slope is, the more time it takes to move between two locations; therefore, steep lines are corresponding to slow movements. (The term "velocity" is often used in time geography, but velocity implies direction while speed is scalar and therefore more appropriate.)

In the real world, individuals' movements are often confined to spatial networks such as those corresponding to transportation systems: these are networks embedded in geographic space with nodes connected to a small number of proximate neighbors. A NTP is a STP constrained by the geometry and speed limits imposed by spatial networks (Miller 1991). Fig. 2 illustrates a NTP

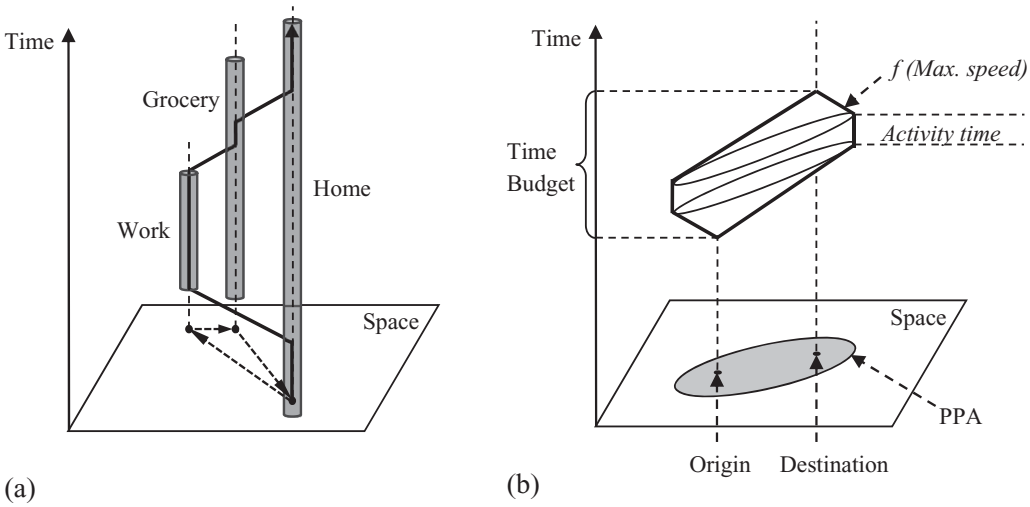

Figure 1. The space-time path (a) and space-time prism (b).

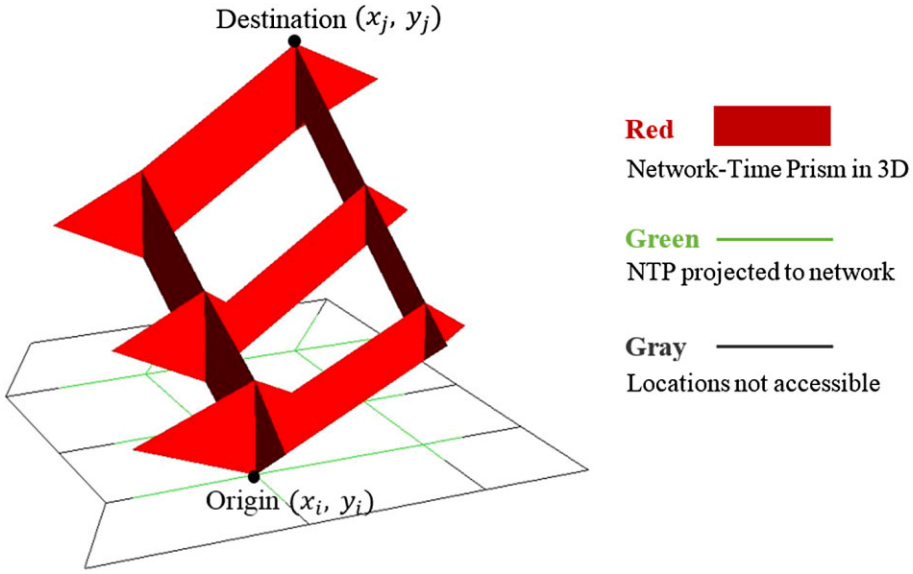

Figure 2. Geometric construction of a NTP.

in two-dimensional space and time from the origin (x_O, y_O) to the destination (x_D, y_D) given the time budget $[t_O, t_D]$ and speed limits within a spatial network ***SN*** (Kuijpers and Othman 2009). Projecting NTP in 3D to the network space, the potential path area (PPA) delimits all accessible locations that are accessible within the networks.

The network locations within the NTP's PPA comprise the following spatial set:

$$g_{OD} = \{(x, y) | t_{SN}((x_O, y_O), (x, y)) + t_{SN}((x, y), (x_D, y_D)) \le t_D - t_O\} \quad (1)$$

where $t_{SN}((x_O, y_O), (x, y))$ and $t_{SN}((x, y), (x_D, y_D))$ denote the minimum travel time from a location (x, y) to the origin (x_O, y_O) and the destination (x_D, y_D), respectively, within the network. The boundaries of the complete NTP (shown as the geometric region in Fig. 2) are determined by the earliest possible arrival time $t^-_{(x,y)}$ and the latest possible departure time $t^+_{(x,y)}$ at each accessible location (x, y) in the NTP PPA:

$$t^-_{(x,y)} = t_O + t_{SN}((x_O, y_O), (x, y)) \quad (2)$$

$$t^+_{(x,y)} = t_D - t_{SN}((x, y), (x_D, y_D)) \quad (3)$$

As an alternative to lower and upper bounds, we can also describe a prism's boundary by delimiting its spatial extent at an instant time within the time interval of its existence (Miller 2005). For a NTP, its spatial extent at a moment in time $t \in [t_O, t_D]$ is (Kuijpers and Othman 2009):

$$Z_{ij}(t) = \{(x, y) | f_O(t) \cap p_D(t) \cap g_{OD}\} \quad (4)$$

$$f_O(t) = \{(x, y) | t_{SN}((x_O, y_O), (x, y)) \le t - t_O\} = \{(x, y) | t^-_{(x,y)} \le t\} \quad (5)$$

$$p_D(t) = \{(x, y) | t_{SN}((x, y), (x_D, y_D)) \le t_D - t\} = \{(x, y) | t^+_{(x,y)} \ge t\} \quad (6)$$

where g_{OD} is the prism's PPA (see equation 1), and fO(t) and pD(t) delimit locations that can be reached from the origin and arrive at the destination at the instant time t, respectively.

Movement probabilities within planar STPs

The proliferation of location-aware technologies such as the global position system and mobile phones has spurred efforts to calculate and visualize realistic prisms using high-resolution mobility data (Neutens, Schwanen, and Witlox 2011; Long and Nelson 2013). Some studies have addressed the properties of activity locations and/or the underlying transportation networks within the prism using georeferenced data (e.g., Kim and Kwan 2003; Geurs and Wee 2004; Kuijpers and Othman 2009; Miller and Bridwell 2009). However, most efforts have focused on delimiting the prism boundary and treating prism-based accessibility as a binary phenomenon: that is, a location at a given time is either inside or outside a prism and therefore accessible or not accessible, respectively. A neglected topic until recently is the properties of the prism interior and their effects on accessibility and other prism outcomes.

A crucial property of the prism interior is the likelihood of visiting different locations within the prism. Intuitively, we should not expect the movement probabilities to be uniform in the prism interior based only on intrinsic prism properties: there are more possible paths proximal to the shortest path connecting the prism anchors and fewer possible paths near the prism boundary. Characterizing the visit probability distribution within a prism enhances its representation of potential mobility, transforming the prism from a binary measure to a more sophisticated accessibility measure that captures variations in path and activity flexibility within its interior (Winter and Yin 2010a, b; Song and Miller 2014).

Winter and Yin (2010a) build a mathematical foundation for modeling the distribution of visit probabilities within planar STPs using RW theory. They start with an undirected RW from the origin and model the individual's movements as a sequence of random steps in two-dimensional discrete space. Based on RW, they conclude that visit probabilities follow a bivariate multinomial distribution at any moment in time. Winter and Yin (2010b) extend the RW approach to take into account the directionality from the origin to the destination. They translate the distribution implied by the undirected RW case to ensure that the highest probabilities are always located along the axis connecting the two prism anchors. They also extend their foundation to the case of continuous space and time, employing the continuous analogy of the bivariate multinomial distribution, that is, the bivariate normal distribution. To incorporate mobility restrictions imposed by the prism, they modify the standard deviation of the distribution and then clip the distribution using the prism boundary. Although their results are intuitive and apparently correct, their argument has three gaps: (1) directionality is imposed at the aggregate level rather than emerging from individual-level movement; (2) the continuous case is based only on analogy from the discrete case; and (3) clipping the bivariate normal distribution is arbitrary and could lead to artifacts.

Song and Miller (2014) extend the work of Winter and Yin (2010a, b) and develop methods for simulating movement probabilities within planar STPs in both discrete and continuous times. For the discrete time and space case, they modify the RW method to capture the directionality imposed by the anchor locations, maximum travel speed, and time budget by dynamically updating the RW movement weights matrix with each time step. For continuous time and space, Song and Miller (2014) develop a method by adopting and modifying the *Brownian Bridge* (BB) approach.

A BB models a continuous stochastic process between two known values; it has been widely applied to analyze phenomena such as asset prices and (more relevantly) animal movements (e.g.,

Lo 1991; Holmes et al. 1994; Karatzas and Shreve 1998; Brillinger et al. 2002; Jonsen et al. 2005, Horne et al. 2007). For two-dimensional BBs, the visit probabilities at any instance in time follow a bivariate normal distribution (Carl and Christopher 2006). This is consistent with Winter and Yin (2010b), but it is based on a fundamental theory of movement rather than an assumption. To restrict BBs within the prism, Song and Miller (2014) apply the concept of a truncated distribution, which is a conditional distribution that confines the domain of some other probability distribution (Johnson, Kotz, and Balakrishnan 1994). A dispersion parameter reflects different levels of mobility within the prism constraints. Provided with movement data collected in the real world, this dispersion parameter can be calibrated to capture an individual's level of mobility within the limits imposed by the prism constraints. The simulated visit probabilities match the intuitive expectations of the unequal distribution and the highest visit probabilities along the axis connecting prism anchors.

Rather than working from movement principles, another approach is to model potential movement using surface generation methods applied to empirical data. Xie and Yan (2008) apply kernel density estimation (KDE) method to the network space in estimating traffic accidents. Downs (2010) further integrates KDE with the STP constraints, and develops a *time-geographic density estimation* (TGDE) method. A set of ordered control points is randomly or regularly selected from the origin to the destination; they constitute the sampled events for the KDE. The kernel function is replaced by the PPA defined by two consecutive control points, and the bandwidth is calculated as the product of the maximum moving speed and the time budget for travel. For movements in the transportation networks, Downs and Horner (2012) develop a network-based TGDE that can generate probabilistic potential path trees given vehicle tracking data. The experimental calculations in both planar and network space illustrate that the TGDE can derive a probabilistic surface for individual's spatial locations at various times.

Methodology

In this section, we discuss the theoretical framework for simulating the visit probabilities within a NTP. We will first provide theoretical background on Markov processes. We will then discuss how to extend these theories to model movement probabilities in the NTPs.

Markov processes

A Markov process is a "memoryless" stochastic process whose future behavior is conditioned on its present status only, and independent of its past history (Paul, Sidney, and Charles 1972; Lawler 2006). The memoryless property facilitates scalable stochastic techniques (Ross 1983, 2009). In social science, Markov processes have been applied to explore and/or model land use dynamics (e.g., Theobald and Hobbs 1998; Verburg and Veldkamp 2005), migrations (e.g., Morrison 1967, 1973; O'Kelly 1979), trip chaining behaviors (e.g., Lerman 1979; O'Kelly 1983; Kondo and Kitamura 1987), and tourism movements (e.g., Xia, Zeephongsekul, and Arrowsmith 2009; Xia, Zeephongsekul, and Packer 2011). These empirical applications demonstrate the practical benefits of Markov techniques in modeling human mobility and dynamics in geographical space with respect to time. They also illustrate the three basic steps of modeling process: (1) selecting the appropriate type of Markov process based on the characteristics of the phenomenon under investigation; (2) defining the status and the state space; and (3) measuring the likelihood to transit from one status to another among all possible statuses in the state space.

The wide variety of Markov processes can be categorized with respect to its time domain or state space. With respect to the time domain T, a Markov process is a *discrete-time* process if T

is a subset of the integers and a *continuous-time* process if T is an interval with positive length (Paul, Sidney, and Charles 1972; Norris 1997). With respect to the state space $\mathcal{S}$, a Markov process can have *finite*, *countable infinite*, or *uncountable infinite* status values (Rosenthal 1995). Given a time domain T and a state space $\mathcal{S}$, a Markov process can be finally defined by the forward equation:

$$\Pr\left(X_{t_{k+1}} = s_{k+1} \mid X_{t_0} = s_0, X_{t_1} = s_1, \ldots, X_{t_k} = s_k\right) = \Pr\left(X_{t_{k+1}} = s_{k+1} \mid X_{t_k} = s_k\right) = p_{s_k s_{k+1}}(t) \quad (7)$$

where X_t denotes the status of a Markov process at time $t \in T$, $\{s_0, s_1, \ldots, s_k\}$ is its status history recorded at the indexed time series $\{t_0, t_1, \ldots, t_k\}$, and $p_{s_k s_{k+1}}(t)$ is the transition probability that measures the likelihood to transit from s_k to s_{k+1} within the time interval $t = t_{k+1} - t_k$.

In Markov process, transitions among statuses are instantaneous: there is no minimum time required to finish a transition. Stochastic processes with time delays before transitions occur are no longer strictly Markovian. However, since they can bring additional flexibility to model a dynamic probabilities system while retaining enough of the memoryless properties, they have been widely accepted as a member of the Markov family and are referred to as *semi-Markov processes* (Howard 1971). Compared with the Markov processes, a semi-Markov process requires an additional function that describes the probability for the process to hold a specific amount of time before transiting from one status to another.

To model movement probabilities within NTPs, we adopt two Markov processes: (1) Brownian motion on graphs (as convergence of a RW on graphs) and (2) continuous-time semi-Markov process. They can both applied to model continuous-time diffusion processes on a graph $G = (V, E)$ with a finite set of vertices $V = \{v_1, v_2, v_3 \ldots\}$ and edges $E = \{e_1, e_2, e_3, \ldots\}$. The graph can be either directed (if edges connected vertex pairs have directions associated with them) or undirected (if both directions are allowed) (Wilkinson 2006).

Brownian motion on graphs

Brownian motion is a continuous-time stochastic process that meets specific conditions regarding independence and normality (Harrison 1985). Leaving the origin 0 (zero) at time t_0, a one-dimensional Brownian motion $B(t)$ has the following properties (Hoel, Port, and Stone 1972; Andrei and Paavo 2002):

i. *initial value*: $B(t_0) = 0$
ii. *continuity*: $\forall t \in [t_0, t_n]: \lim_{x \to t} B(x) = B(t)$
iii. *independent increments (Markovian)*: for any time series $t_0 < t_1 < \ldots < t_n < \infty$, the increments $B(t_1) - B(t_0)$, $B(t_2) - B(t_1)$, $\ldots$, $B(t_n) - B(t_{n-1})$ are independent
iv. *stationarity and normality*: for $0 \le t < s < \infty$, $B(s) - B(t) \sim \mathcal{N}\left(0, (s-t)\sigma^2\right)$

Considering a RW within edges of an undirected graph, for each step, the object jumps from any point location x on an edge to the points ε distance away (but also on an edge) with equal probabilities. After an appropriate rescaling, such RWs weakly converge to Brownian motion on graphs (Enriquez and Kifer 2001). Brownian motion on a graph is a diffusion process that when starts on an edge e_k, the process within the edge is equivalent to one-dimensional Brownian motion on the interval e_k (Kostrykin, Potthoff, and Schrader 2012) and prescribes a natural rule for probabilities of jumps over the end vertex (or vertices respectively) (Baxter and Chacon 1984).

Continuous-time semi-Markov process

For a directed graph, each edge has a direction associated with it; therefore, $e_{12} : v_1 \rightarrow v_2$ is different from $e_{21} : v_2 \rightarrow v_1$ and the object may only be able to jump "forward" along an edge. In this case, Brownian motion on graphs discussed above does not apply and we can adopt continuous-time semi-Markov processes instead.

A continuous-time semi-Markov process consists of an imbedded Markov process with transition probabilities and a holding time density function associated with each transition (Howard 1971). The transition probability p_{ij} describes the likelihood that the process will make its next transition to state j given that the last transition was to state i (see equation 7). The process is time homogeneous if the transition probabilities $\{p_{ij}\}$ do not change over time, and is time inhomogeneous otherwise (Hoem 1972; Platis, Limnios, and Le Du 1998).

The holding time density function $h_{ij}(\tau)$ describes the probability that one transition from i to j will take τ amount of time; it can be any probability density function (PDF) that is right continuous (Howard 1971), such as the exponential distribution:

$$h_{ij}(\tau) = \lambda_{ij} e^{-\lambda_{ij}\tau} \quad \tau \geq 0 \tag{8}$$

where λ_{ijl} is an indicator of how fast the system can leave state i through the transition to state j. Its cumulative density function (CDF) ${}^{\leq}h_{ij}(t)$ is the probability that the process will arrive at j no later than t, and its complementary CDF ${}^{>}h_{ij}(t)$ is the probability of arriving later than t:

$${}^{\leq}h_{ij}(t) = \int_0^t h_{ij}(\tau)\, d\tau = 1 - e^{-\lambda_{ij} t} \quad \tau \geq 0 \tag{9}$$

$${}^{>}h_{ij}(t) = \int_t^\infty h_{ij}(\tau)\, d\tau = e^{-\lambda_{ij} t} \quad \tau \geq 0 \tag{10}$$

The set of $p_{ij}(\tau) = p_{ij} \times h_{ij}(\tau)$ composite core matrix $P(\tau)$ is the basic descriptor of the continuous-time semi-Markov process (Howard 1971). We will now discuss how to adopt and extend Brownian motion and continuous-time semi-Markov processes to model visit probabilities within NTPs for two movement types.

Modeling movement probabilities within NTP

We represent transportation network as a graph $G = (V, E)$, with road intersections as a set of vertices $V = \{v_1, v_2, v_3, \ldots\}$, road segments as a set of edges $E = \{e_{ij}\}$, and distance expressed in travel time between two end vertices as $t_{ij} = t_{SN}(v_i, v_j)$. We model visit probabilities in NTPs for nonvehicular movement (e.g., walking) using Brownian motion since this type of mobility is loosely constrained by the network and can occur in any direction within the network geometry. For vehicular movement such as bicycling and driving, we model NTP visit probabilities using continuous-time semi-Markov processes since this type of movement is constrained by direction and speed limits that may vary by edge (due to legal speed limits or congestion). Our fundamental assumption is that higher visit probabilities are associated with more potential space-time paths and therefore greater flexibility.

Movement probabilities for the nonvehicular mobility

There are three factors we need to consider for modeling movement within NTPs. First, due to the time budget $t \in [t_O, t_D]$, we should not directly use properties of classic Brownian

motion theory derived based on $t \in [0, \infty)$. Second, due to the maximum moving speed, accessible locations are bounded in a finite area at any time, so the standard normal distribution needs to be modified. Third, due to the pressure to arrive at the destination before scheduled time, the distribution of movement probabilities is expected to have a bias toward the destination.

We model the probability of moving along an edge e_{ij} at $t \in [t_O, t_D]$ as the joint probability of that edge being reached from the origin within $(t - t_O)$ and arriving at the destination within $(t_D - t)$. This edge probably describes, after leaving the origin, how likely the object is moving along the edge e_{ij} at time t among all accessible edges at that time. For an undirected graph, we have $e_{ij} = e_{ji}$ and four types of movements along edges according to the entrance and exit vertices for each edge (see Fig. 3): (1) $v_i \rightarrow v_j$, (2) $v_i \rightarrow v_i$, (3) $v_j \rightarrow v_i$, and (4) $v_j \rightarrow v_j$.

We use the earliest arrival time t_i^- and latest departure time t_i^+ at a vertex v_i to indicate potential space-time paths and define Brownian motion from the origin and to the destination, respectively:

$$B(t) - B(t_O) \sim \mathcal{N}\left(0, (t - t_O)(\sigma(t - t_O))^2\right) \tag{11}$$

$$B(t_D) - B(t) \sim \mathcal{N}\left(0, (t_D - t)(\sigma(t_D - t))^2\right) \tag{12}$$

where $\sigma(\Delta t) = \delta \times \sqrt{\Delta t}$ is the variance dependent on Δt and includes a dispersion parameter δ describing the mobility level of the object within the space-time constraints. Since the independent increments are depended only on the time interval Δt, they are stationary and retain fundamental properties of the Brownian motion. Then, we derive the probability for vertex $v_i : \left(t_i^-, t_i^+\right)$ as:

$$\varphi\left(B\left(t_i^-\right)\right) = \begin{cases} 0, & t_i^- > t \\ \dfrac{1}{\sqrt{2\pi} \times \delta \times (t - t_O)} e^{-\frac{\left(t_i^- - t_O\right)^2}{2\delta^2 (t - t_O)^2}}, & t_i^- \le t \end{cases} \tag{13}$$

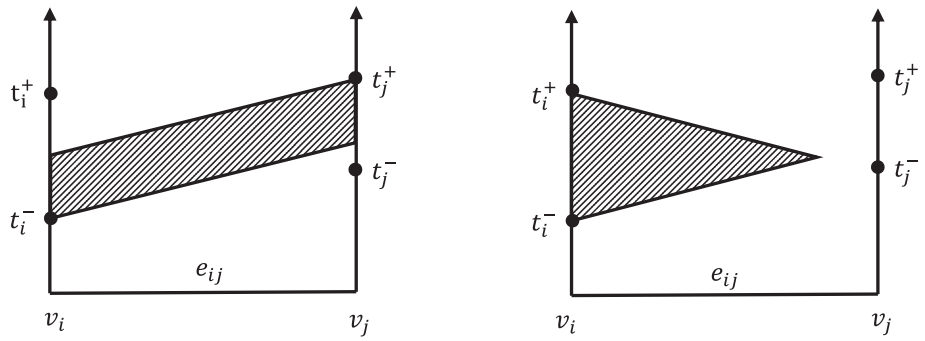

(a) from v_i to its adjacent v_j (move through an edge)

(b) from v_i back to itself (U-turn within an edge)

Figure 3. Two of the four types of movement between adjacent vertices: (1) move through an edge, and (2) U-turn within an edge (the other two types are symmetric).

$$\varphi\left(B\left(t_i^+\right)\right)=\begin{cases}0, & t_i^+ < t\\ \dfrac{1}{\sqrt{2\pi}\times\delta\times\left(t_D-t\right)}e^{-\frac{\left(t_D-t_i^+\right)^2}{2\delta^2\left(t_D-t\right)^2}}, & t_i^+ \geq t\end{cases} \tag{14}$$

and the probability to move from v_i to v_j is given by

$$P_{ij}(t)=\begin{cases}\varphi\left(B\left(t_i^-\right)\right)\times\varphi\left(B\left(t_j^+\right)\right), & t_i^- + t_{ij} \leq t_j^+\\ 0, & \text{otherwise}\end{cases} \tag{15}$$

The probability of moving along e_{ij} is the sum of all four types of movements. In addition, we normalize the edge probabilities so that, for any time $t \in [t_O, t_D]$, they add up to unity. This is because, for the movement within a NTP, its location at any instant time can only be along those accessible edges and nowhere else. Therefore, edge probabilities e_{ij} are

$$P\left(e_{ij}, t\right)=\frac{\sum_{k=i,j,l=i,j}P_{kl}(t)}{\sum_{e_{mn}\in E}P\left(e_{mn}, t\right)} \tag{16}$$

Movement probabilities for vehicular mobility

For vehicle-based movements, speed limits, one-way and turn restrictions imposed by transportation networks make it impossible for vehicles to move back and forth freely. Therefore, instead of modeling movement probabilities using Brownian motion, we adopt theories of continuous-time Markov process that account for both probabilities and hold time for transitions. We modify the classic theories considering two factors. First, due to the speed limit, there is a minimum time required to finish transition along each edge. Second, due to the pressure of reaching the destination on time, the conditional transition probabilities $\{p_{ij}(t)\}$ are time inhomogeneous and conditioned on the time $t \in [t_O, t_D]$.

We define a state as a movement starting from vertex v_i to v_j along a linked edge e_{ij} that has not arrived at v_j yet. If $v_j = v_i$, the movement makes a U-turn within the edge e_{ij}; if the movement arrives at v_j and turns back to v_i, this is considered two consecutive states. The state space is all possible movements between vertex pairs in transportation network, which is finite in reality. We adopt and modify an exponential distribution for holding time density function (Johnson et al. 1994):

$$h_{ij}(\tau)=\begin{cases}\lambda e^{-\lambda\left(\tau-t_{ij}\right)}, & \tau \geq t_{ij}\\ 0, & \tau < t_{ij}\end{cases} \tag{17}$$

where $t_{ij} = t_{RN}(v_i, v_j)$ is the minimum transition time derived based on the length and speed limit of the edge e_{ij}, and λ is the transition rate on the basis of the mobility level provided by the transportation network. The extra time available for movement is $\Delta\tau = \tau - t_{ij}$; hence, the PDF is:

$$h_{ij}(\Delta\tau)=\begin{cases}\lambda e^{-\lambda\Delta\tau}, & \Delta\tau \geq 0\\ 0, & \Delta\tau < 0\end{cases} \tag{18}$$

which can also be interpreted as the probability to reach v_j with arrival time $(t_{ij} + \Delta\tau)$.

Considering one-way and turn restrictions, we represent transportation network as a directed graph. We first derive the time profile for each edge e_{ij}, $\left(t_i^-, t_j^+, t_{ij}\right)$ and use it as indicator of

potential arrival times and departure times at end vertices. We first consider a diffusion process from the origin: the probability to pass a location within network is dependent on the available arrival times at that location. Since the arrival times follow the exponential distribution with rate λ, the probability that the movement can reach e_{ij} from v_i can be derived:

$$p_{O\to i}(t)=\begin{cases} 0, & t\in\left[t_O,t_i^-\right) \\ \int_{t_i^-}^{t}\lambda e^{-\lambda\tau}d\tau=e^{-\lambda t_i^-}-e^{-\lambda t}, & t\in\left[t_i^-,t_j^+-t_{ij}\right) \\ \int_{t_i^-}^{t_j^+-t_{ij}}\lambda e^{-\lambda\tau}d\tau=e^{-\lambda t_i^-}-e^{-\lambda\left(t_j^+-t_{ij}\right)}, & t\in\left[t_j^+-t_{ij},t_D\right] \end{cases} \tag{19}$$

Similarly, we can derive the probability of reaching the destination from v_j based on available departure times:

$$p_{j\to D}(t)=\begin{cases} 0, & t\in\left[t_j^+,t_D\right] \\ \int_{t_D-t_j^+}^{t_D-t}\lambda e^{-\lambda\tau}d\tau=e^{-\lambda\left(t_D-t_j^+\right)}-e^{-\lambda(t_D-t)}, & t\in\left[t_i^-+t_{ij},t_j^+\right) \\ \int_{t_D-t_j^+}^{t_D-t_i^--t_{ij}}\lambda e^{-\lambda\tau}d\tau=e^{-\lambda\left(t_D-t_j^+\right)}-e^{-\lambda\left(t_D-t_i^--t_{ij}\right)}, & t\in\left[t_O,t_i^-+t_{ij}\right) \end{cases} \tag{20}$$

The probability for movement $(v_i \to v_j : e_{ij})$ at t is derived based on flexibilities provided by two ends, and normalized so that, for any $t \in [t_O, t_D]$, probabilities for state space add up to unity.

$$P\left(v_i\to v_j:e_{ij},t\right)=\frac{p_{O\to i}(t)\times p_{j\to D}(t)}{\sum_{e_{mn}\in E}P\left(e_{mn},t\right)},\ t_i^-+t_{ij}\le t_j^+ \tag{21}$$

Implementation and results

Software tools and study area

We implement the methodology using the programming language Python and three modules that are supported by Python: (1) NumPy for creating and managing large-size arrays; (2) SciPy that provides basic statistic functions (e.g., PDF for the normal distribution); and (3) ArcPy (the site package provided with ESRI ArcGIS software) for conducting network analysis and visualizing results. We develop and manage the functions, classes, and modules using Eclipse: this is a multilanguage software development environment designed for large-scale project development and featured by its extensible plug-in systems (interpreters) including Python.

The analysis in this article uses transportation network and GPS data for New York City, USA. We choose New York City because of the availability of GPS data collected by a commercial navigation vendor (TomTom, Inc.). We choose Manhattan specifically since it allows us to

use locations such as bridge and tunnel exits and entrances as surrogates for the NTP anchor points. The transportation network data set used is *U.S. and Canada Cartographic Streets* downloadable from ESRI ArcGIS online resources. This data set represents detailed streets, interstate highways, and major roads within the United States and Canada. For privacy consideration, the GPS data provided by TomTom, Inc. correspond to only a subset of the entire population, and all demographic information has been removed from the original data set. The sample area covers New York County and parts of Bronx, Queens, and Kings Counties in the state of New York, and part of Hudson and Bergen Counties in the state of New Jersey. There are approximately 136,000 vehicle trajectories collected within a two-week period available in the data set. The original data were preprocessed so that off-road movements have been removed and the raw GPS fixes have been map-matched to the transportation networks data set used by TomTom navigation devices (Stogios, Mahmassani, and Vovsha 2013). The final data provided to us are second-by-second GPS locations along each trajectory with longitude, latitude, and time stamp information that we map-matched to the *U.S. and Canada Cartographic Streets* networks.

Scenario 1: walking within Manhattan

For nonvehicle movements, we will discuss a simple but illustrative scenario based on walking in Manhattan, New York City (see Fig. 4). We construct the NTP using local streets with sidewalks as the spatial network and do not assign direction restrictions to street segments. We choose an origin-destination pair in midtown Manhattan to maximize variations in route choices. The Euclidean distance between the origin and the destination is approximately 2,500 meter, the time budget is set as 15 min, and the maximum walking speed is set as 112 meter/min according to adult walking speed (Bohannon 1997).

We first calculate the network time distance (in minutes) from the origin and to the destination and use it to derive a time profile between each pair of adjacent vertices. We then derive the probability to move from v_i to v_j along edge e_{ij} at any time t within the time budget. Fig. 4 shows the probabilities for each edge at selected time points. Fig. 4 also includes the planar space PPA boundary for comparison purposes. As can be seen, the method generates movement probabilities that are intuitive and consistent with planar STP interior movement probabilities,

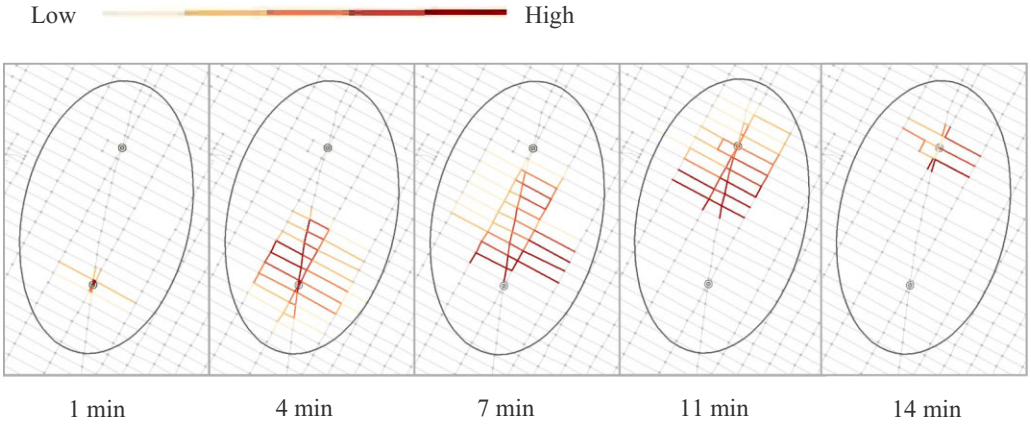

Figure 4. Simulated NTP visit probabilities based on walking within 15 min, aggregated by network edge (planar space PPA overlaid for reference).

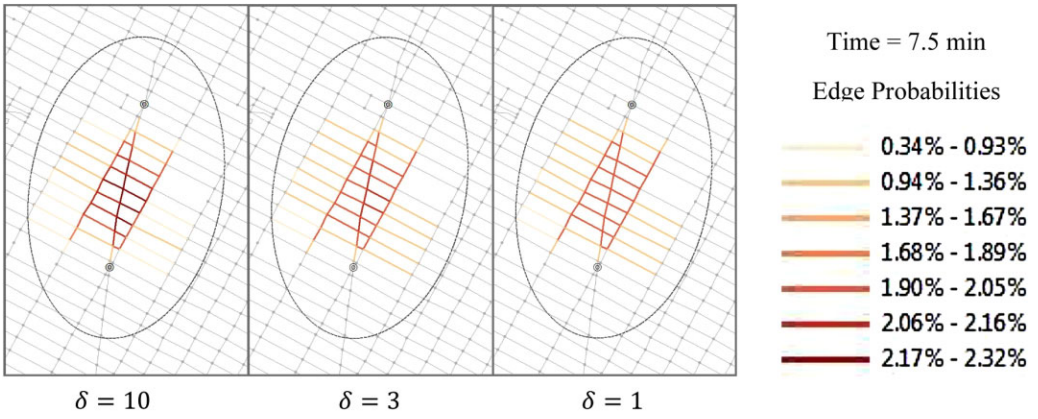

Figure 5. Simulated NTP visit probabilities under varying dispersion parameter values δ.

albeit impacted by the network configuration. (The NTP appears to extend beyond the boundary of the planar PPA at 11 min, but this is due to aggregating probabilities to the entire network edge.)

As discussed in the third section, the NTP Brownian motion process contains a dispersion parameter δ that shapes the visit probability distribution based on the level of mobility within the NTP constraints. Although we do not have empirical walking data to calibrate this parameter, we can illustrate its effects on the NTP visit probability distribution; see Fig. 5. A higher value for δ corresponds to a lower mobility level: this generates a more concentrated visit probability distribution. A smaller δ corresponds to higher mobility levels: this generates a more dispersed visit probability distribution.

Scenario 2: driving across Manhattan

For vehicular movement, we examine a more complex case based on driving across Manhattan. Given the information available for the transportation network, we derive the time profile for each edge accounting for varying speed limits within the network as well as turn delays at intersections. We first illustrate the calibration of the transition rate parameter λ; we continue with a comparison of simulated visit probability distributions with empirical distributions derived from GPS data.

We define two NTPs: (1) using the Holland Tunnel and the Manhattan Bridge on the west and east sides of Manhattan as prism anchors, modeling potential mobility across southern Manhattan with a 25-min time budget; and (2) using the Third Avenue Bridge and the Queensborough Bridge (a.k.a. 59th Street Bridge) on the east side of Manhattan as prism anchors, modeling potential mobility across eastern Manhattan given a time budget of 40 min.

Calibrating transition rate parameter

In order to calibrate the transition rate parameter λ, we select three routes that contain multiple sample trajectories within each NTP and calibrate the transition rate using ordinary least squares. All three sets of data indicate that the transition rate is 0.003 in the Manhattan area (in time units of seconds). The mean square error between CDF estimated by holding time density function and

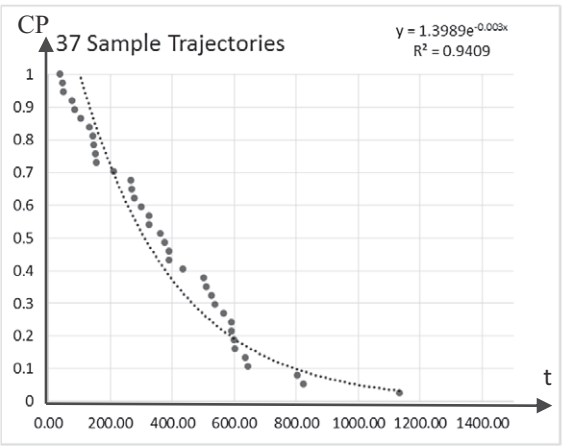

CP = cumulative probability

t = travel time (s)

Figure 6. Sample trajectories along one route from Holland Tunnel to Manhattan Bridge.

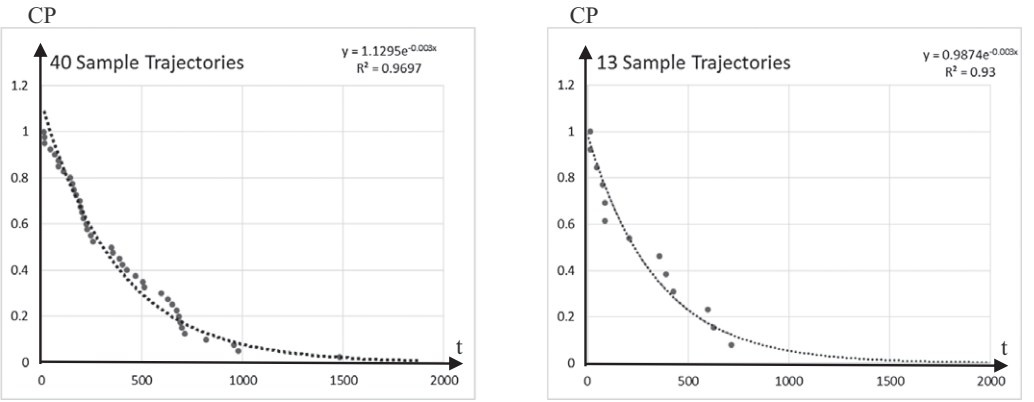

Figure 7. Sample trajectories along two routes from 3rd Avenue Bridge to 59th Street Bridge.

the empirical probabilities represented by CDF are 0.0168, 0.0097, and 0.0046 for three sample sets (Figs. 6 and 7) which indicate a good fit. We use this transition rate value in the simulations below.

Comparing empirical and simulated visit probabilities

We first examine the southern Manhattan (Holland Tunnel-Manhattan Bridge) NTP. After selecting GPS trajectories that enter Manhattan through the Holland Tunnel and leave via the Manhattan Bridge, we match these traces to the underlying road network using the Network Analyst extension provided by ArcGIS. Fig. 8 shows the map-matched 72 GPS trajectories in southern Manhattan that exit the Holland Tunnel on the left and enter the Manhattan Bridge on the right. The color of each edge indicates the number of trajectories passing through it within the entire time frame; the most frequently used route is along the dark red one, which is longer in distance than the light red route toward the axis connecting this Origin-Destination pair but has fewer turns and therefore less potential time cost.

Since the time interval between GPS locations is not uniform along traces and no information is available between two consecutive GPS locations, we do not attempt to estimate the

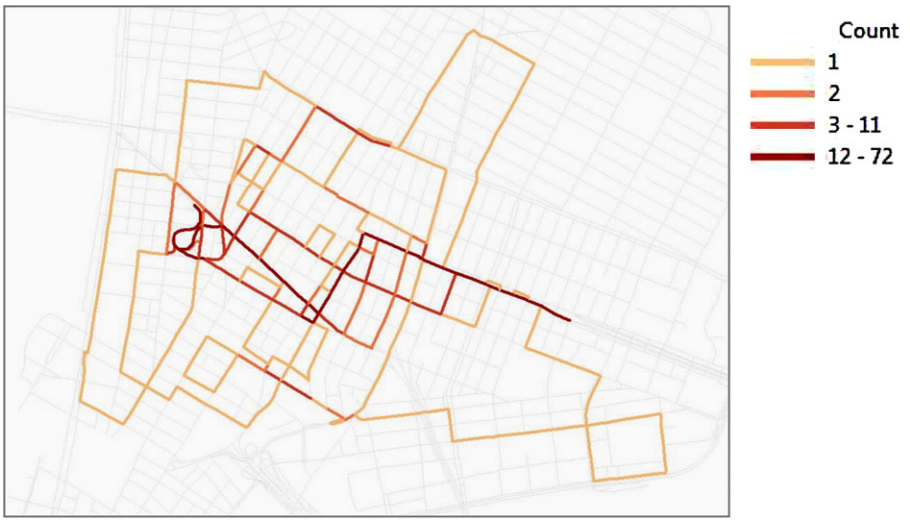

Figure 8. Empirical edge count frequencies for southern Manhattan NTP.

object's precise location at a time point $t \in [t_O, t_D]$, but instead generate the empirical visit probability for entire edges at a given time. We first select the pair of consecutive locations ($Pt1$, $Pt2$) where the time stamp at $Pt1$ is not later than the given time T and time stamp at $Pt2$ is not earlier than T. Then, we overlay the part of the map-matched trace $\overrightarrow{Pt1Pt2}$ with the network edges and assign values to overlapped edges based on the percentage of $Pt1Pt2$ along each overlapped edge. For instance, if $Pt1Pt2$ has 10% along $E1$, 60% along $E2$, and the rest 30% along $E3$, the values assigned to $E1$, $E2$, and $E3$ are 0.1, 0.6, and 0.3, respectively. The empirical visit probability for each edge is calculated by adding up values from all traces overlapping that edge and dividing by the total number of traces. Since the maximum travel time for these 72 traces is 23.558 min, we use 25 min (1,500 s) as the time budget in the previous section for theoretical visit probability distribution.

Fig. 9 shows the derived empirical distributions of visit probabilities at selected moments in time. One minute after departure, most traces are still on ramps exiting the Holland Tunnel, and there are variations on selecting the specific tunnel exit. Three minutes after departure, most traces are going through major roads toward the destination; apparently quicker routes have higher probabilities than detours. Five minutes after departure, the distribution becomes dispersed and probabilities increase along edges that deviate from the axis connecting the origin and destination. Twenty minutes after departure, only 13 traces are still on their way; the others have already passed the entrance to the Manhattan Bridge.

After examining the lingering 13 traces, it is interesting to note that, although in general traces along apparently shorter/quicker route take less time than routes with detours, the trace with the highest cost is along the most frequently used route (see the route in dark red at 20 min after departure in Fig. 8) and the time spent along that route varies from 5.2 min to more than 23.3 min. A reasonable explanation is that the most frequently used route is likely to have higher traffic volumes than others, especially during peak traffic hours.

To simulate the visit probabilities within the NTP, we first derive the earliest arrival time from the origin and the latest departure time toward the destination for each vertex based on driving time and turn costs. We calculate the driving time based on the geometric length and the

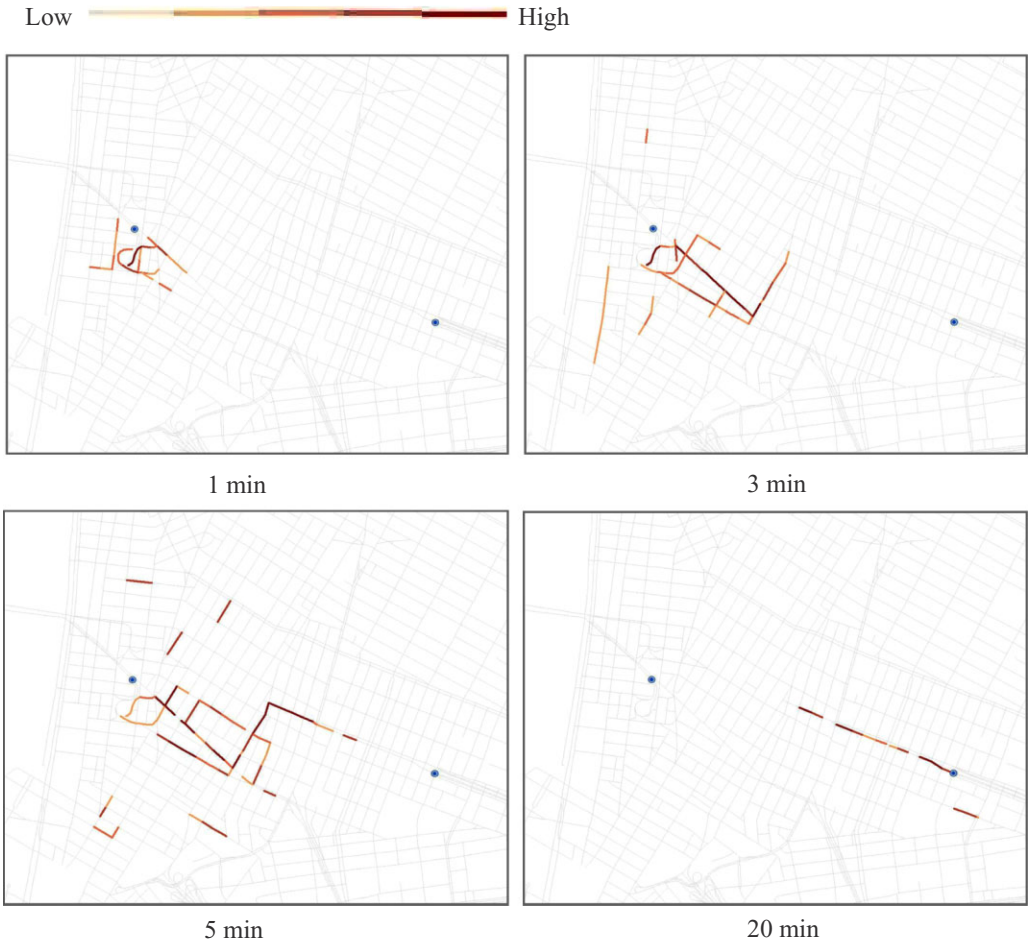

Figure 9. Empirical visit probabilities along edges for southern Manhattan NTP.

speed limit of each road segment. We also consider one-way restrictions and turn costs at intersections (3 s for right turns, 15 s for left turns, and 40 s for U-turns). Fig. 10 shows the results at the same selected moments in time as in Fig. 9, with the simulated distributions on the top compared with the empirical distributions on the bottom. Since the number of accessible edges changes across time, we adopt the quantile classification method so that each class contains an equal number of edges.

Although the simulated and empirical distributions in Fig. 10 seem dissimilar at first glance, this is partly due to the simulated probabilities corresponding to a population but the empirical probabilities being only a small sample of that population. Accounting for these differences, the distributions match each other well based on visual inspection. For example, at the first minute, it is highly likely that vehicles are still on the ramp; at the third minute, the detour at the yellow edge derived from the empirical data matches the skew of higher probabilities around the origin (in orange); at the fifth minute, most trips navigate toward the destination; at the 20th minute, it is possible for traces to be entering the Manhattan Bridge, and high probabilities are along quicker routes and skewed to the bridge entrance. (We also conduct a quantitative comparison below.)

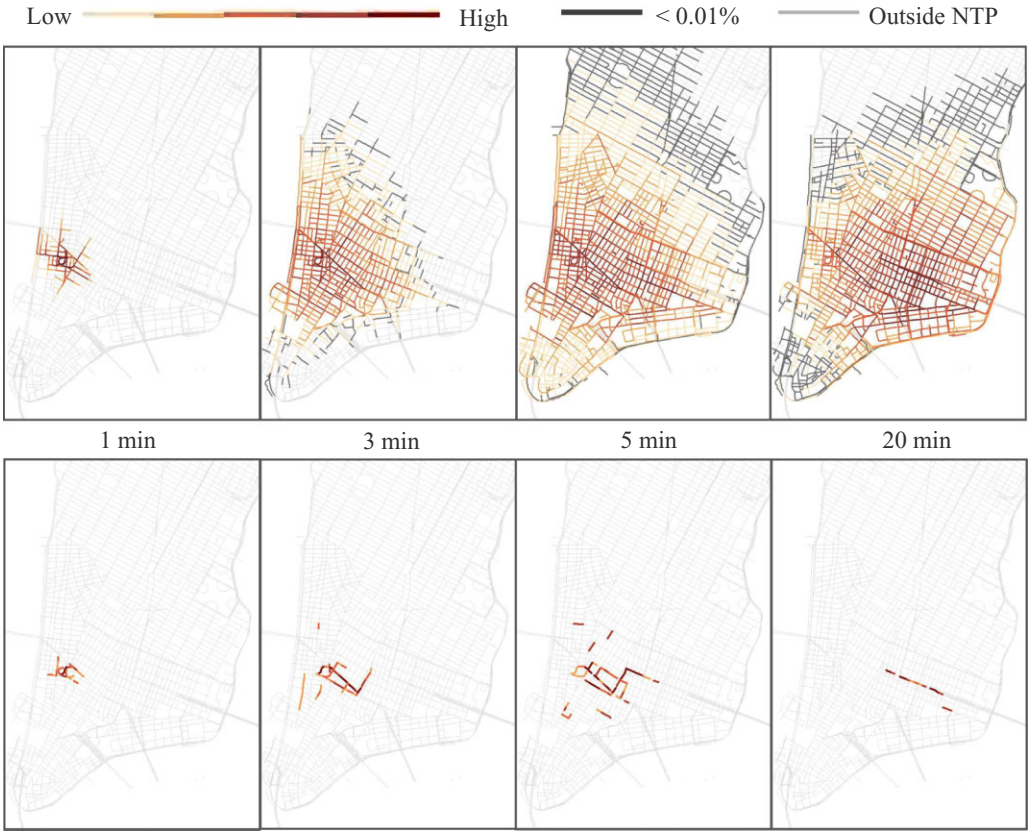

Figure 10. Comparison of simulated and empirical visit probabilities for the southern Manhattan scenario.

Another property to note in Fig. 10 is the dark gray edges: these are theoretically within the NTP but have a very low visit probability (less than 0.01%). This illustrates that a binary NTP can be an overestimation of accessibility since it includes edges that are unlikely to be visited. The visit probabilities provide a more realistic and nuanced depiction of accessibility than a traditional NTP.

We also define a second NTP for movements in eastern Manhattan from the Third Avenue Bridge to the Queensborough Bridge with a 40-min time budget and compare simulated visit probabilities with empirical probabilities derived from 104 GPS trajectories. Fig. 11 illustrates the edge count frequency. The most frequently used routes are indicated in dark red; these are generally along Franklin D. Roosevelt (East River) Drive (FDR). There are variations in route selection, especially after exiting the limited-access highway near the destination.

Fig. 12 shows the derived empirical visit probabilities at selected moments in time. Three minutes after departure, traces have left the Third Avenue Bridge and traces along FDR go further in distance than those taking local roads. At the fifth minute, some traces exit FDR and take local roads instead. At the tenth minute, almost one-fourth of traces taking FDR have entered the Queensborough Bridge, while traces taking local roads are only halfway to that destination. As time goes on, variations become more significant, especially for traces exiting FDR at exit 12 connecting the Queensborough Bridge. At 25th minute, only 17 traces are still on their way

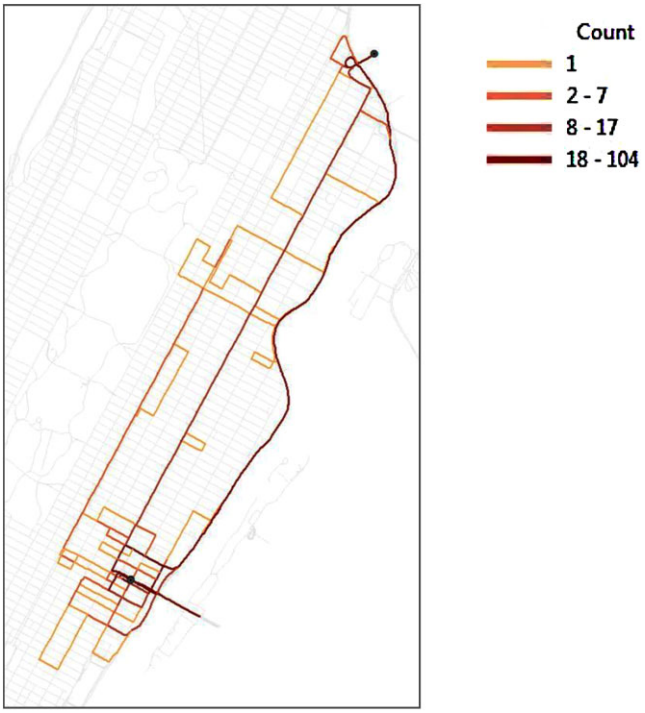

Figure 11. Empirical edge count frequencies for eastern Manhattan scenario.

toward the destination, and similar to the first NTP, likely due to the delay along FDR. Delay seems to be common along FDR across a tunnel between 81st and 89th streets, which may due to both a reduction in the speed limit and traffic entering FDR at 79th street toward south.

Using the same settings for driving times and turn costs as in the southern Manhattan NTP, we simulate visit probabilities at selected times and compare these to the empirical visit probabilities. Fig. 13 illustrates this comparison. The simulated visit probabilities indicate that, as time goes on, accessible edges and high visit probabilities move toward the destination. Compared with the empirical distribution, edges along quicker routes are more likely to be chosen at any time in the simulated distribution. It is worth pointing out that the high visit probabilities along some east-west local roads are due to their allowance of two-way traffic. Once again, note from Fig. 13 the substantial overestimation of accessibility provided by a binary NTP: dark gray arcs are theoretically within the NTP but are unlikely to be visited.

Table 1 provides results from calculating the root mean square error (RMSE) to quantitatively measure the difference between the simulated and empirical visit probability distributions. We use two bases for comparison: (1) the estimated NTP and (2) the empirical GPS traces. The former allows us to assess the accuracy of the simulated visit probabilities with respect to the empirical visit probabilities. For this purpose, we first select edges $\{e_{ij}\}^t$ within NTP at time t and calculate the visit probabilities for them $\left\{SimP_{(e_{ij},t)}\right\}$. Then, we derive the empirical visit probabilities for selected edges $\{e_{ij}\}^t$ based on GPS traces, $\left\{EmpP_{(e_{ij},t)}\right\}$. Given the number of edges $Cnt(t)$, the RMSE at time t is calculated as:

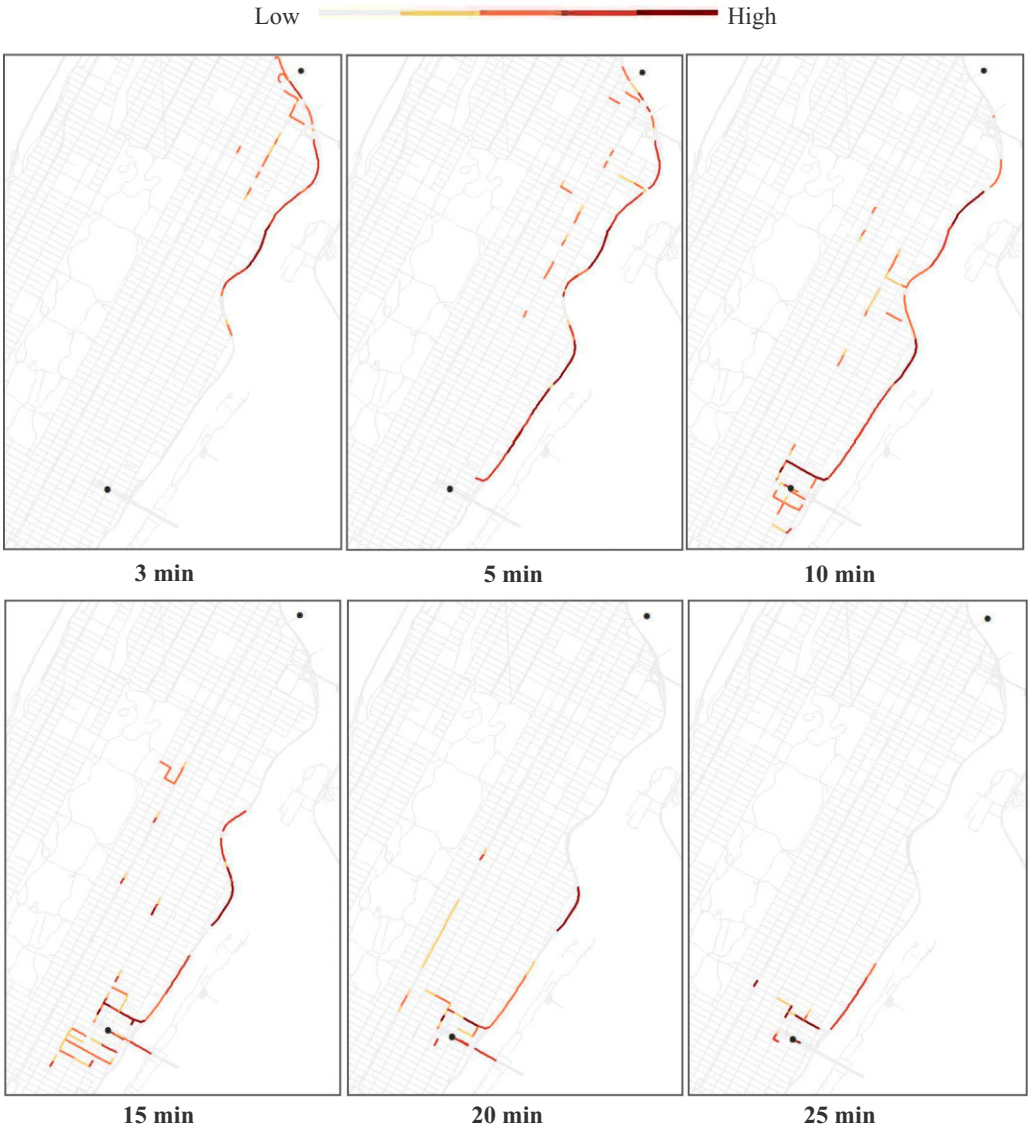

Figure 12. Empirical visit probabilities for eastern Manhattan scenario.

$$RMSE^{1}(t) = \frac{\sum_{\{e_{ij}\}^{t}} \left(EmpP_{(e_{ij},t)} - SimP_{(e_{ij},t)} \right)^{2}}{Cnt(t)} \tag{22}$$

The latter allow us to examine how well the simulated visit probabilities fit the empirical routes. For this purpose, we further refine the edges $\{e_{ij}\}^{t}$ to those that have been used by at least one GPS trace throughout the entire time period, and use them to simulate the visit probabilities. This can be seen as the case when a set of empirical routes is predetermined and variations exist in the actual selection of an empirical route as well as the movements along the selected route. The calculation of RMSE is similar to the first case.

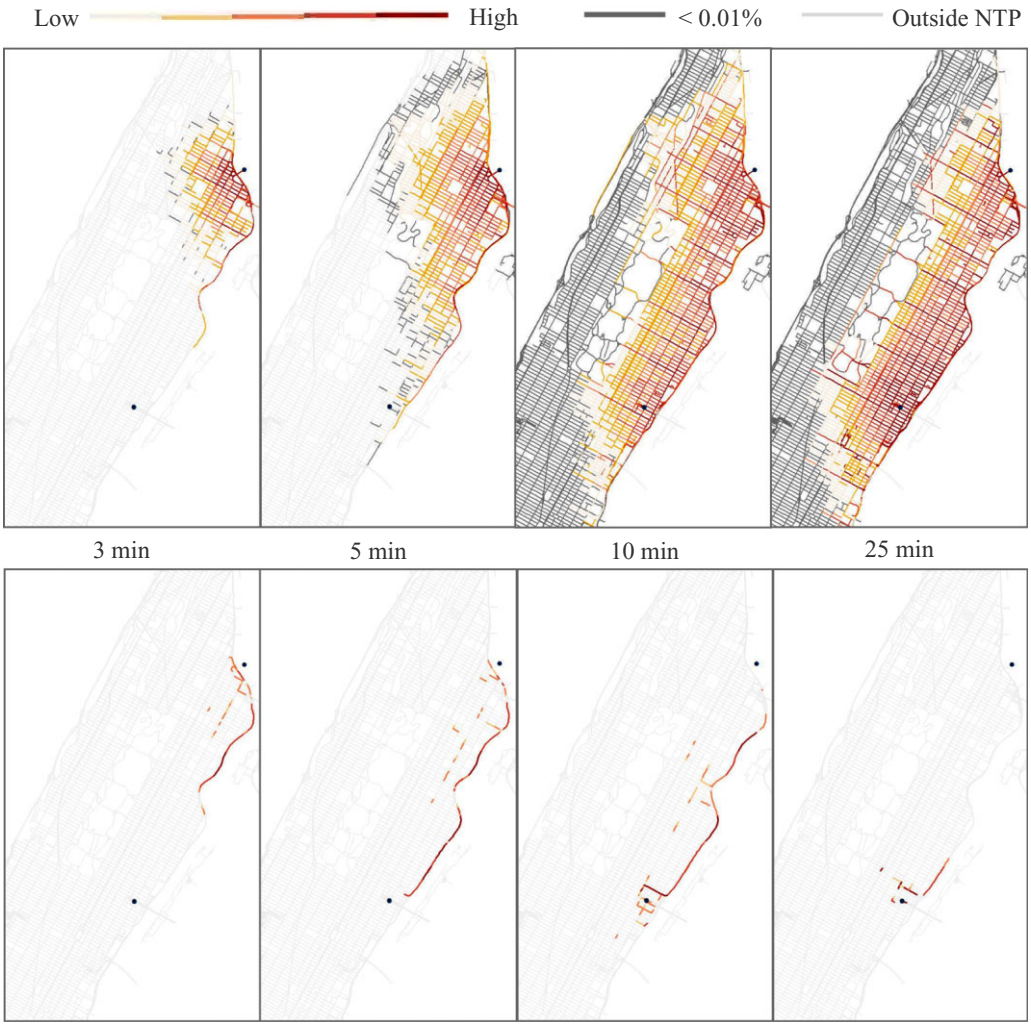

Figure 13. Comparison of simulated (top) and empirical (bottom) visit probabilities for the eastern Manhattan scenario.

Table 1 Root Mean Square Error between Simulated and Empirical Distribution at Selected Time

(a) Southern Manhattan scenario

Base	5 min	10 min	15 min	20 min
NTP	3.05%	0.26%	0.48%	2.47%
Empirical traces (n = 72)	1.06%	1.39%	2.60%	1.70%

(b) Eastern Manhattan scenario

Base	5 min	10 min	15 min	20 min	25 min	30 min	35 min
NTP	0.51%	0.21%	0.24%	0.30%	0.33%	1.10%	6.60%
Empirical traces (n = 104)	1.73%	0.93%	1.20%	1.45%	1.64%	2.94%	5.97%

Table 1 provides the RMSE results. Fit is poorest in the initial time periods when travelers have the most amount of flexibility, becomes better over time, and becomes poorer again toward the end of the NTP time interval, likely owing to varying arrival times at the second anchor. But the differences between the simulated and empirical distributions are relatively small, indicating an overall good fit between the simulated and empirical NTP visit probability distributions.

Conclusion

Methods for simulating visit probabilities within the NTP continue the development of an analytical framework for time geography and improve the sophistication of the STP as a measure of potential mobility and accessibility. In this article, we develop a framework to modeling movement probabilities within the NTP interior using two Markovian techniques. For nonvehicular mobility, we adopt Brownian motion on graphs and introduce the dispersion parameter to capture the individual mobility level within prism constraints. For vehicular mobility, we adopt continuous-time semi-Markov process and calibrate the transition rate to capture the network mobility level. Visit probabilities for both types are simulated based on the fundamental assumption that higher visit probabilities are associated with more potential space-time paths determined by the earliest arrival time from the origin and the latest departure time toward the destination at each vertex. To illustrate these two methods, we simulate visit probabilities using Python and ArcPy on the platform Eclipse, and visualize results using ESRI ArcGIS. The distribution of visit probabilities for nonvehicular mobility matches our intuitive expectations and allows us to incorporate the individual mobility level using a dispersion parameter. Results for vehicular mobility show that, regardless of the small sample size (72 and 104 GPS trajectories), the simulated distributions are visually and statistically consistent with the empirical distributions within the study area of Manhattan, New York City.

The current work could be extended by obtaining additional data. TomTom, a commercial vendor, provided the data used to validate vehicular mobility, and vehicles' movements may be guided by the navigation device, GPS trajectories that are not related to a navigation service could enhance the validation results. In particular, we may see a wider dispersion of routes within the NTP with less bias toward major roads. For nonvehicle mobility, data on pedestrians' movements between activity locations could be used to derive empirical distributions that could be compared with the simulated visit probabilities. In addition, more detailed data on the transportation network (e.g., empirical travel times on road segments, the distribution and timing of traffic signals) could improve the accuracy of simulated visit probabilities for vehicular mobility.

Another extension of this article is to use NTP visit probability distributions to refine prism-based accessibility measures (Kwan 1998; Miller 1999). As the results in this article indicate, a binary conceptualization of the prism can be a substantial overestimation of accessibility since it includes locations that are theoretically within the prism but unlikely to be visited. At the very least, a visit probability distribution can be used to circumscribe the NTP to eliminate unlikely locations based on a probability threshold. In addition, it is possible to weight the opportunities within a NTP based on visit probabilities. For example, the widely used cumulative opportunities measure of accessibility in transportation planning (Wachs and Kumagai 1973; Hanson and Schwab 1987; El-Geneidy and Levinson 2006) could be enhanced by weighting opportunities by visit probabilities to develop probabilistic accessibility measures.

Another extension of this research could be to incorporate other models of mobility behavior to derive the NTP visit probabilities. The Markovian techniques used in this article estimate visit probabilities based on the intrinsic properties of the prism independent of any behavioral model, although parameters allow the probability distribution to be calibrated to observed movement behavior. However, it is possible to use techniques such as agent-based modeling to estimate NTP visit probabilities based on different behaviors and trip purposes. This could enhance the flexibility of the probabilistic NTP for different types of applications in transportation policy and planning. It would also be illuminating to compare intrinsic prism visit probability distributions with the extrinsic distributions provided through prism-constrained behavioral models.

More generally, a probabilistic approach to the NTP can improve its functionality as a measure of accessibility costs in addition to benefits. A major factor affecting mobility cost is the speed of the vehicle: among other things, higher speeds lead to greater fuel consumptions, higher tailpipe emissions, higher risk of accidents, and greater consequences if an accident occurs (Shibata and Fukuda 1994; Barth et al. 1996; Ahn et al. 2002). Note that the distribution of possible speeds varies by location in the prism: there is a greater range of potential speeds toward the center of prism relative to the boundary where only the maximum speed is possible. The NTP visit probabilities could be used to weight the possible speeds to derive the expected speed-related cost of the prism. This can be used to estimate speed-related properties of the prism such as the expected fuel consumption and tailpipe emissions implied by a prism. In addition, the methods in our article could be used to estimate the expected accidents or consequences such as death rates implied by a prism, all else being equal.

Acknowledgement

This research was supported by the National Science Foundation (NSF) through grant number BCS-1224102. The analysis was based on data provided by Strategic Highway Research Program SHRP-2 project L04.

References

Ahn, K., H. Rakha, A. Trani, and M. Van Aerde. (2002). "Estimating Vehicle Fuel Consumption and Emissions Based on Instantaneous Speed and Acceleration Levels." *Journal of Transportation Engineering* 128(2), 182–90.

Andrei, N. B., and S. Paavo. (2002). *Handbook of Brownian Motion—Facts and Formulae*, 2nd ed. Basel and Boston: Birkhäuser Verlag.

Barth, M., F. An, J. Norbeck, and M. Ross. (1996). "Modal Emissions Modeling: A Physical Approach." *Transportation Research Record: Journal of the Transportation Research Board* 1520(1), 81–8.

Baxter, J. R., and R. V. Chacon. (1984). "The Equivalence of Diffusions on Networks to Brownian Motion." *Contemporary Mathematics* 26, 33–47.

Bohannon, R. W. (1997). "Comfortable and Maximum Walking Speed of Adults Aged 20–79 Years: Reference Values and Determinants." *Age and Ageing* 26(1), 15–9.

Bowman, J. L., and M. E. Ben-Akiva. (2001). "Activity-Based Disaggregate Travel Demand Model System with Activity Schedules." *Transportation Research Part A: Policy and Practice* 35(1), 1–28.

Brillinger, D. R., H. K. Preisler, A. A. Ager, J. G. Kie, and B. S. Stewart. (2002). "Employing Stochastic Differential Equations to Model Wildlife Motion." *Bulletin of the Brazilian Mathematical Society* 33(3), 385–408.

Carl, E. R., and K. I. W. Christopher. (2006). *Gaussian Processes for Machine Learning*. Cambridge, MA: MIT Press.

Dong, X., M. E. Ben-Akiva, J. L. Bowman, and J. L. Walker. (2006). "Moving from Trip-Based to Activity-Based Measures of Accessibility." *Transportation Research Part A: Policy and Practice* 40(2), 163–80.

Downs, J. A. (2010). "Time-Geographic Density Estimation for Moving Point Objects." In *Geographic Information Science*, 16–26, edited by S. I. Fabrikant, T. Reichenbacher, M. van Kreveld, and C. Schlieder. Berlin and Heidelberg: Springer, LNCS 6292.

Downs, J. A., and M. W. Horner. (2012). "Probabilistic Potential Path Trees for Visualizing and Analyzing Vehicle Tracking Data." *Journal of Transport Geography* 23, 72–80.

El-Geneidy, A. M., and D. M. Levinson. (2006). Access to Destinations: Development of Accessibility Measures (No. MN/RC-2006-16). Minnesota Department of Transportation, Research Services Section.

Ellegård, K., and U. Svedin. (2012). "Torsten Hägerstrand's Time-Geography as the Cradle of the Activity Approach in Transport Geography." *Journal of Transport Geography* 23, 17–25.

Enriquez, N., and Y. Kifer. (2001). "Markov Chains on Graphs and Brownian Motion." *Journal of Theoretical Probability* 14(2), 495–510.

Geurs, K. T., and B. V. Wee. (2004). "Accessibility Evaluation of Land-Use and Transport Strategies: Reviews and Research Directions." *Journal of Transport Geography* 12(2), 127–40.

Hägerstrand, T. (1970). "What about People in Regional Science?" *Papers of the Regional Science Association* 24(1), 6–21.

Hanson, S., and M. Schwab. (1987). "Accessibility and Intra-Urban Travel." *Environment and Planning A* 19, 735–48.

Harrison, J. M. (1985). *Brownian Motion and Stochastic Flow Systems*. New York: Wiley.

Hoel, P., S. Port, and C. Stone. (1972). *Introduction to Stochastic Processes*. Boston, MA: Houghton Mifflin.

Hoem, J. M. (1972). "Inhomogeneous Semi-Markov Processes, Select Actuarial Tables, and Duration-Dependence in Demography." In *Population Dynamics*, 251–296, edited by T.N.E. Greville. New York: Academic.

Holmes, E. E., M. A. Lewis, J. E. Banks, and R. R. Veit. (1994). "Partial Differential Equations in Ecology: Spatial Interactions and Population Dynamics." *Ecology* 75(1), 17–29.

Horne, J. S., E. O. Garton, S. M. Krone, and J. S. Lewis. (2007). "Analyzing Animal Movements Using Brownian Bridges." *Ecology* 88(9), 2354–63.

Howard, R. A. (1971). *Dynamic Probabilistic Systems, Volume II: Semi-Markov and Decision Processes, Vol. 2*. New York: Wiley & Sons, Inc.

Johnson, N. L., S. Kotz, and N. Balakrishnan. (1994). *Continuous Univariate Distribution, Vol. 1 (Wiley Series in Probability and Statistics)*. New York: Wiley-Interscience, NYSE: JWA.

Jonsen, I. D., J. M. Flemming, and R. A. Myers. (2005). "Robust State-Space Modeling of Animal Movement Data." *Ecology* 86(11), 2874–80.

Karatzas, I., and S. E. Shreve. (1998). *Methods of Mathematical Finance*, Vol. 39. New York: Springer.

Kim, H. M., and M. P. Kwan. (2003). "Space-Time Accessibility Measures: A Geocomputational Algorithm with a Focus on the Feasible Opportunity Set and Possible Activity Duration." *Journal of Geographical Systems* 5(1), 71–91.

Kondo, K., and R. Kitamura. (1987). "Time-Space Constraints and the Formation of Trip Chains." *Regional Science and Urban Economics* 17, 49–65.

Kostrykin, V., J. Potthoff, and R. Schrader. (2012). "Brownian Motions on Metric Graphs." *Journal of Mathematical Physics* 53(9), 095206–095236.

Kuijpers, B., and W. Othman. (2009). "Modeling Uncertainty of Moving Objects on Road Networks Via Space-Time Prisms." *International Journal of Geographical Information Science* 23(9), 1095–117.

Kwan, M. P. (1998). "Space-Time and Integral Measures of Individual Accessibility: A Comparative Analysis Using a Point-Based Framework." *Geographical Analysis* 30(3), 191–216.

Lawler, G. F. (2006). *Introduction to Stochastic Process*, 2nd ed. London: CRC Press.

Lenntorp, B. (1977). "Paths in Space-Time Environments: A Time Geographic Study of Movement Possibilities of Individuals." *Environment and Planning* 9(8), 961–72.

Lerman, S. R. (1979). "The Use of Disaggregate Choice Models in Semi-Markov Process Models of Trip Chaining Behavior." *Transportation Science* 13(4), 273–91.

Lo, A. W. (1991). "Long-Term Memory in Stock Market Prices." *Econometrica* 59(5), 1279–313.

Long, J. A., and T. A. Nelson. (2013). "A Review of Quantitative Methods for Movement Data." *International Journal of Geographic Information Science* 27(2), 292–318.

McNally, M. G. (2000). "The Activity-Based Approach." In *Handbook of Transport Modelling*, 53–69, edited by D. A. Hensher and K. J. Button. Amsterdam: Pergamon.

Miller, H. J. (1991). "Measuring Accessibility Using Space-Time Prism Concepts within Geographic Information Systems." *International Journal of Geographical Information System* 5(3), 287–301.

Miller, H. J. (1999). "Measuring Space-Time Accessibility Benefits within Transportation Networks: Basic Theory and Computational Methods." *Geographical Analysis* 31, 187–212.

Miller, H. J. (2005). "A Measurement Theory for Time Geography." *Geographical Analysis* 37(1), 17–45.

Miller, H. J., and S. A. Bridwell. (2009). "A Field-Based Theory for Time Geography." *Annals of the Association of American Geographers* 99, 49–75.

Morrison, P. A. (1967). "Duration of Residence and Prospective Migration: The Evaluation of A Stochastic Model." *Demography* 4(2), 553–61.

Morrison, P. A. (1973). "Theoretical Issues in the Design of Population Mobility Models." *Environment and Planning* 5(1), 125–34.

Neutens, T., T. Schwanen, and F. Witlox. (2011). "The Prism of Everyday Life: Towards a New Research Agenda for Time Geography." *Transport Reviews* 31(1), 25–47.

Norris, J. R. (1997). *Markov Chains*, 1st ed. Cambridge: Cambridge University Press.

O'Kelly, M. E. (1979). "Two Models of Canadian Interregional Migration." *Canadian Journal of Regional Science II* 2, 59–80.

O'Kelly, M. E. (1983). "Multipurpose Shopping Trips and the Size of Retail Facilities." *Annals of the Association of American Geographers* 73(2), 231–9.

O'Sullivan, D., A. Morrison, and J. Shearer. (2000). "Using Desktop GIS for the Investigation of Accessibility by Public Transport: An Isochrones Approach." *International Journal of Geographical Information Science* 14(11), 85–104.

Paul, G. H., C. P. Sidney, and J. S. Charles. (1972). *Introduction to Stochastic Processes*. Boston, MA: Houghton Mifflin.

Platis, A., N. Limnios, and M. Le Du. (1998). "Hitting Time in a Finite Non-Homogeneous Markov Chain with Applications." *Applied Stochastic Models and Data Analysis* 14(3), 241–53.

Pred, A. (1977). "The Choreography of Existence: Comments on Hagerstrand's Time Geography and Its Usefulness." *Economic Geography* 53, 207–21.

Rosenthal, J. S. (1995). "Minorization Conditions and Convergence Rates for Markov Chain Monte Carlo." *Journal of the American Statistical Association* 90(430), 558–66.

Ross, S. M. (1983). *Stochastic Processes*. New York: Wiley & Sons Ltd.

Ross, S. M. (2009). *Introduction to Probability and Statistics for Engineers and Scientists*. Boston: Academic Press.

Shibata, A., and K. Fukuda. (1994). "Risk Factors of Fatality in Motor Vehicle Traffic Accidents." *Accident Analysis & Prevention* 26(3), 391–7.

Song, Y., and H. J. Miller. (2014). "Simulating Visit Probability Distributions within Planar Space-Time Prisms." *International Journal of Geographical Information Science* 28(1), 104–25.

Stogios, Y. C., H. Mahmassani, and P. Vovsha. (2013). Incorporating Reliability Performance Measures in Operations and Planning Modeling Tools: Final Report (SHRP 2 Reliability Project L04). Transportation Research Board (TRB).

Theobald, D. M., and N. T. Hobbs. (1998). "Forecasting Rural Land-Use Change: A Comparison of Regression and Spatial-Based Models." *Geographical and Environmental Modeling* 2, 65–82.

Thrift, N., and A. Pred. (1981). "Time-Geography: A New Beginning." *Progress in Human Geography* 5(2), 277–86.

Verburg, P. H., and A. Veldkamp. (2005). "Introduction to the Special Issue on Spatial Modeling to Explore Land Use Dynamics: Editorial." *International Journal of Geographical Information Science: IJGIS* 19(2), 99–102.

Wachs, M., and T. G. Kumagai. (1973). "Physical Accessibility as a Social Indicator." *Socio- Economic Planning Sciences* 7, 437–56.

Wilkinson, D. J. (2006). *Stochastic Modelling for Systems Biology*. BocaRaton: Chapman & Hall/CRC.

Winter, S., and Z. C. Yin. (2010a). "The Elements of Probabilistic Time Geography." *Geoinformatica* 15(3), 417–34.

Winter, S., and Z. C. Yin. (2010b). "Directed Movements in Probabilistic Time Geography." *International Journal of Geographical Information Science* 24(9), 1349–65.

Xia, J. C., P. Zeephongsekul, and C. Arrowsmith. (2009). "Modelling Spatio-Temporal Movement of Tourists Using Finite Markov Chains." *Mathematics and Computers in Simulation* 79(5), 1544–53.

Xia, J. C., P. Zeephongsekul, and D. Packer. (2011). "Spatial and Temporal Modelling of Tourist Movements Using Semi-Markov Processes." *Tourism Management* 32(4), 844–51.

Xie, Z., and J. Yan. (2008). "Kernel Density Estimation of Traffic Accidents in a Network Space." *Computers, Environment and Urban Systems* 32(5), 396–406.